Electronic Supplementary Material (ESI) for Journal of Materials Chemistry A.

Supplementary Information

The Relationship between Oxide-Ion Conductivity and Cation Vacancy Order in the Hybrid Hexagonal Perovskite $Ba_3VWO_{8.5}$

Asma Gilane [a, b], Sacha Fop [a], Falak Sher [b], Ronald I. Smith[c] and Abbie C. Mclaughlin *[a],

[a] The Chemistry Department, University of Aberdeen, Meston Walk, Aberdeen AB24 3UE,
United Kingdom.
E-mail: a.c.mclaughlin@abdn.ac.uk

[b] Department of Chemistry and Chemical Engineering, SBA School of Science and
Engineering, Lahore University of Management Sciences (LUMS), Lahore, Pakistan.
E-mail: fsher@lums.edu.pk

[c] ISIS Facility, STFC Rutherford Appleton Laboratory, Harwell Campus, Didcot, OX11 0QX,
United Kingdom

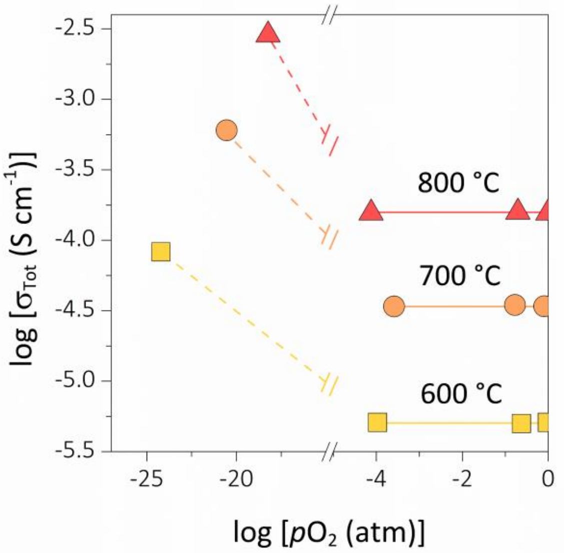

Figure S1. Dependence of the total conductivity of $Ba_3WVO_{8.5}$ against the oxygen partial pressure.

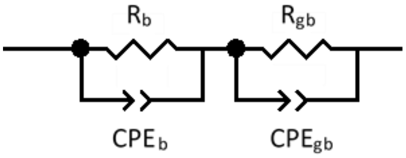

Figure S2. Equivalent circuit model employed for analysis of the $Ba_3VWO_{8.5}$ impedance data collected under dry air; R indicates a resistor, while CPE is a constant phase element.

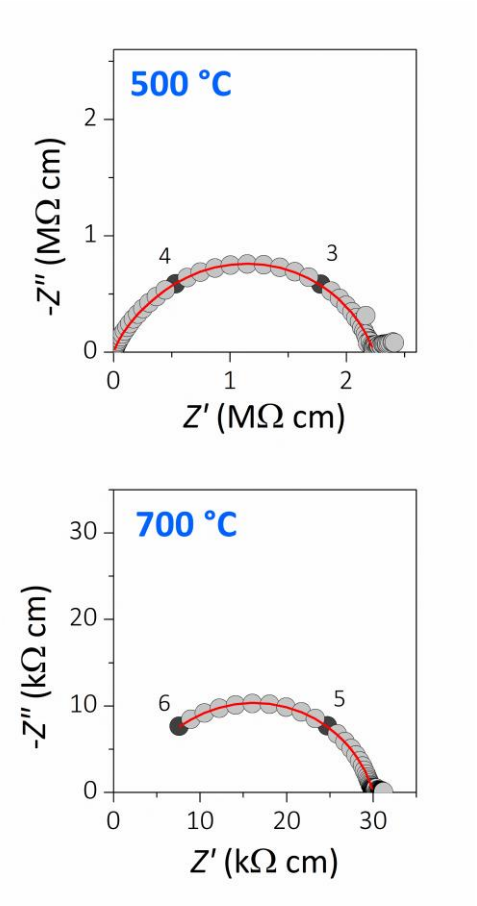

Figure S3. Representative equivalent circuit fit of complex impedance plots of $Ba_3VWO_{8.5}$ recorded in dry air at 500 °C and 700 °C. The numbers and corresponding filled circles indicate selected frequency decades; the red line is the equivalent circuit fitting.

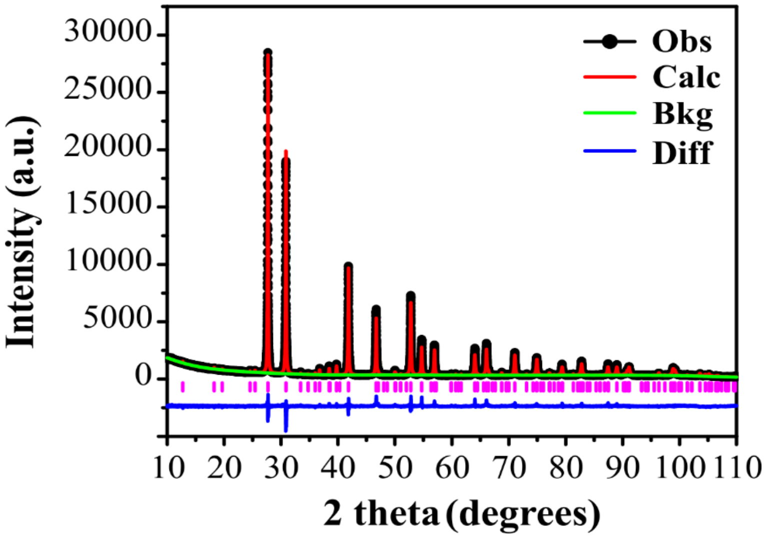

Figure S4. Fitted X-ray diffraction histogram of $Ba_3WVO_{8.5}$ at room temperature.

Table S1: Refined atomic parameters from Rietveld fit of the $R\bar{3}m$ H model from powder X-ray diffraction data. The oxygen occupancies were fixed in the refinement. The M1 site is composed of 50% V and 50% W.

ATOM	SITE	X	Y	Z	FRACTION	U_{ISO} (Å^2)
BA1	**3*a***	0	0	0	1	0.0141 (6)
BA2	**6*c***	0	0	0.20721(2)	1	0.0141 (9)
M1	**6*c***	0	0	0.39834(4)	1	0.0168 (2)
O1	**18*h***	0.1756(3)	0.8244(3)	0.1003(1)	1	0.0261 (7)
O2	**9*e***	0.5	0	0	0.448	0.0261 (7)
O3	**6*c***	0	0	0.3313(3)	0.577	0.0261 (7)

Data were refined in space group $R\bar{3}m$ *H* with χ^2 = 2.93, R_p = 4.10%, R_{wp} = 5.55%; refined unit cell parameters; *a* = *b* = 5.822215(1) Å, *c* = 21.13536(7) Å, *V* = 620.450(4) Å^3.

Table S2: Selected bond distances and angles for Ba$_3$VWO$_{8.5}$. M indicates W/V.

Bond distance (Å^2)		**Bond angle (°)**	
Ba1–O1	2.7694 (4)	**O1–M1–O1**	99.53 (5)
Ba1–O2	2.91127 (3)	**O1–M1–O3**	126.32 (19) 107.62 (9) 119.67 (20)
Ba1–O3	3.1011 (22)	**O1–M1–O2**	86.373 (12) 170.77 (7)
Ba2–O1	2.8215 (7) 2.95763 (14)	**O2–M1–O2**	86.93 (5)
Ba2–O2	3.1560 (6)		
Ba2–O3	2.5444 (12)		
M1–O1	1.8378 (8)		
M1–O2	2.1160 (9)		
M1–O3	1.4551 (19)		

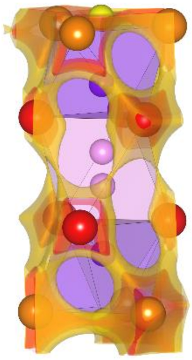

Figure S5. Bond-valence site energy map calculated for $Ba_3NbWO_{8.5}$. Darker colors indicate the lower isosurface levels (< 0.9 eV over the global minimum), while the lighter colours are for the highest isosurface levels (between 1.0 eV and 1.6 eV over the global minimum).

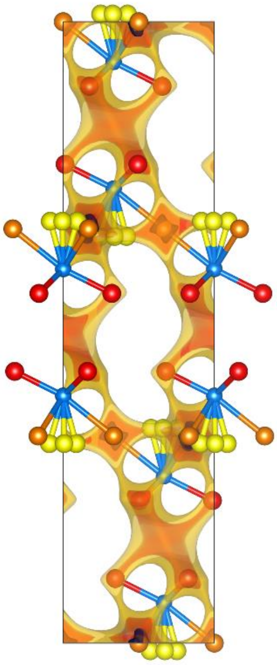

Figure S6. Bond-valence site energy map calculated for $Ba_3NbMoO_{8.5}$ with the M2 occupancy set to zero, to give a M1-vac-M1 stacking. Darker colors indicate the lower isosurface levels (< 0.5 eV over the global minimum), while the lighter colours are for the highest isosurface levels (between 0.7 eV and 1.4 eV over the global minimum).

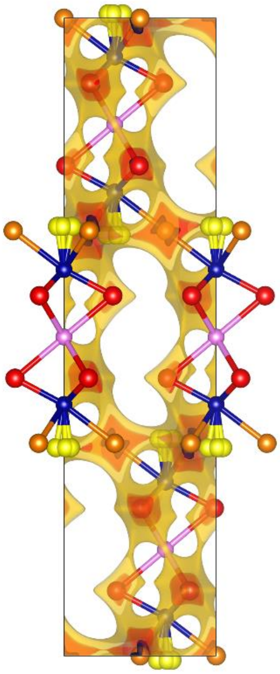

Figure S7. Bond-valence site energy map calculated for $Ba_3VWO_{8.5}$ with the M1 occupancy set to 0.9 and the M2 occupancy set to 0.1, to give the hybrid metal stacking. This BVSE map demonstrates that the O1-O1 connectivity (with relative barrier of 1.470 eV) along the edges of the M2O16 octahedra is re-established when the M2 site is occupied. Interestingly, the relative barrier for the O1-O2 pathway segment is also reduced to 0.690 eV. Darker colors indicate the lower isosurface levels (< 0.5 eV over the global minimum), while the lighter colours are for the highest isosurface levels (between 0.65 eV and 1.6 eV over the global minimum).